

Caenorhabditis elegans *lin-35*/Rb, *efl-1*/E2F and Other Synthetic Multivulva Genes Negatively Regulate the Anaphase-Promoting Complex Gene *mat-3*/APC8

David Garbe,¹ Jeffrey B. Doto¹ and Meera V. Sundaram²

Department of Genetics, University of Pennsylvania, Philadelphia, Pennsylvania 19104-6100

Manuscript received December 31, 2003

Accepted for publication March 12, 2004

ABSTRACT

Retinoblastoma (Rb)/E2F complexes repress expression of many genes important for G₁-to-S transition, but also appear to regulate gene expression at other stages of the cell cycle. In *C. elegans*, *lin-35*/Rb and other synthetic Multivulva (SynMuv) group B genes function redundantly with other sets of genes to regulate G₁/S progression, vulval and pharyngeal differentiation, and other unknown processes required for viability. Here we show that *lin-35*/Rb, *efl-1*/E2F, and other SynMuv B genes negatively regulate a component of the anaphase-promoting complex or cyclosome (APC/C). The APC/C is a multisubunit complex that promotes metaphase-to-anaphase progression and G₁ arrest by targeting different substrates for ubiquitination and proteasome-mediated destruction. The *C. elegans* APC/C gene *mat-3*/APC8 has been defined by temperature-sensitive embryonic lethal alleles that strongly affect germline meiosis and mitosis but only weakly affect somatic development. We describe severe nonconditional *mat-3* alleles and a hypomorphic viable allele (*ku233*), all of which affect postembryonic cell divisions including those of the vulval lineage. The *ku233* lesion is located outside of the *mat-3* coding region and reduces *mat-3* mRNA expression. Loss-of-function alleles of *lin-35*/Rb and other SynMuv B genes suppress *mat-3*(*ku233*) defects by restoring *mat-3* mRNA to wild-type levels. Therefore, Rb/E2F complexes appear to repress *mat-3* expression.

THE retinoblastoma (Rb) protein is an important tumor suppressor and regulator of gene expression (for reviews see HARBOUR and DEAN 2000; STEVAUX and DYSON 2002). Rb itself does not bind DNA; instead it binds to E2F transcription factors and recruits corepressor complexes to E2F target promoters, thereby repressing gene transcription. Some E2F proteins function as transcriptional activators in the absence of Rb, while other E2F proteins serve only as corepressors with Rb. Rb/E2F complexes inhibit G₁-to-S phase progression by repressing target genes such as cyclin E and cyclin A (DEGREGORI *et al.* 1995; OHTANI *et al.* 1995; SCHULZE *et al.* 1995; REN *et al.* 2002). Rb/E2F complexes also regulate targets important for other stages of the cell cycle and for differentiation (LUKAS *et al.* 1999; DAHIYA *et al.* 2001; FAY *et al.* 2003). For example, microarray and chromatin immunoprecipitation experiments have identified spindle checkpoint genes and other mitotic genes as likely targets of E2F (ISHIDA *et al.* 2001; MULLER *et al.* 2001; REN *et al.* 2002; DIMOVA *et al.* 2003). However, the functional importance of these mitotic targets is not understood.

The anaphase-promoting complex or cyclosome (APC/C) is a multisubunit E3 ubiquitin ligase that plays

multiple roles in cell-cycle progression (HARPER *et al.* 2002; PETERS 2002). For example, in conjunction with the regulatory subunit Cdc20/Fizzy (Fzy) the APC/C targets anaphase inhibitors such as Pds1/securin for destruction and thus allows metaphase-to-anaphase transition during meiosis and mitosis (DAWSON *et al.* 1995; SIGRIST *et al.* 1995; VISINTIN *et al.* 1997). In conjunction with a different regulatory subunit, Cdh1/Fizzy-related (Fzr), the APC/C targets mitotic cyclins for destruction and thus inhibits G₁-to-S progression (SIGRIST and LEHNER 1997; VISINTIN *et al.* 1997). The APC/C is therefore important for both mitotic progression and G₁ arrest.

In *Caenorhabditis elegans*, cell-cycle regulation by Rb/E2F and by the APC/C has often been studied in the context of vulval development (FURUTA *et al.* 2000; BOXEM and VAN DEN HEUVEL 2001). Vulval development involves stereotypical patterns of cell division that give rise to a total of 22 vulval descendants (Figure 1; WANG and STERNBERG 2001). Reduced or increased proliferation is easily detected in this tissue. Because vulval divisions occur relatively late in larval development (after maternally provided gene products have decayed), the vulva is one of the tissues most commonly affected in cell-cycle mutants. Vulval development is also controlled by several oncogene signaling pathways, including Ras, Wnt, and Notch pathways (WANG and STERNBERG 2001), and thus provides a convenient system to test how these signaling pathways coordinately influence cell fate patterning and cell-cycle progression.

C. elegans *lin-35*/Rb and *efl-1*/E2F function redundantly

¹These authors contributed equally to this work.

²Corresponding author: Department of Genetics, University of Pennsylvania, 446A Clinical Research Bldg., 415 Curie Blvd., Philadelphia, PA 19104-6145. E-mail: sundaram@mail.med.upenn.edu

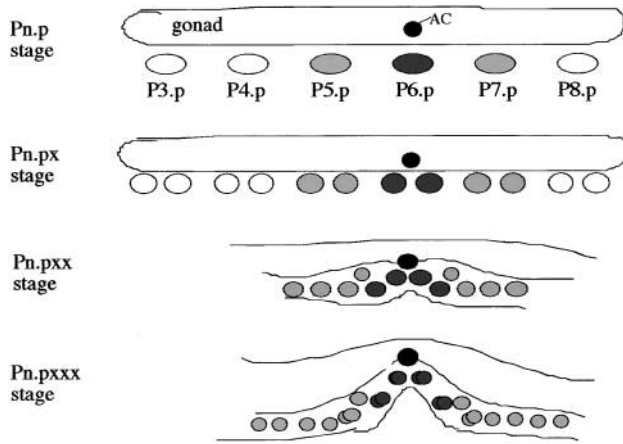


FIGURE 1.—Stages of vulval development. The vulval precursor vells (VPCs) P3.p–P8.p all divide to generate Pn.px daughters. VPCs that have been induced to adopt a vulval fate (P5.p, P6.p, and P7.p) undergo two additional rounds of division to generate at total of 22 Pn.pxxx nuclei (SULSTON and HORVITZ 1977; SULSTON and WHITE 1980).

with other genes to control multiple aspects of development. First, *lin-35/Rb* and *efl-1/E2F* function redundantly with other cell-cycle regulators to inhibit G₁-to-S progression of vulval and other cells. For example, although *lin-35/Rb* mutations alone do not cause obvious cell-cycle defects, they cause hyperproliferation in an *fzr-1* (*Fzr*) mutant background (FAY *et al.* 2002) and enhance the hyperproliferative defects of *cki-1,2* (cyclin kinase inhibitor) mutants (BOXEM and VAN DEN HEUVEL 2001). Second, *lin-35/Rb* and *efl-1/E2F* genes belong to a larger group of “synthetic multivulva” (SynMuv) genes, two sets of genes that function redundantly to inhibit Ras-mediated vulval fate induction (FERGUSON and HORVITZ 1989; LU and HORVITZ 1998; CEOL and HORVITZ 2001). Mutations in class A or class B SynMuv genes have little or no effect on vulval development, but class A/class B double mutants have excess vulval induction (multivulva phenotype), as do activated Ras pathway mutants. *lin-35/Rb* and *efl-1/E2F* are class B SynMuv genes and appear to inhibit vulval gene expression (LU and HORVITZ 1998; CEOL and HORVITZ 2001), although direct targets of these genes have not yet been identified. Finally, *lin-35/Rb* seems to have additional essential (but redundant) roles since a variety of mutations have been found to cause synthetic lethality in a *lin-35/Rb* mutant background (FAY *et al.* 2002, 2003).

Mutations in several *C. elegans* APC/C subunits have been identified in screens for temperature-sensitive maternal-effect lethal mutants that arrest at the one-cell stage (FURUTA *et al.* 2000; GOLDEN *et al.* 2000; DAVIS *et al.* 2002; RAPPLEYE *et al.* 2002; SHAKES *et al.* 2003). These include *emb-27* (APC6/Cdc16), *emb-30* (APC4), *mat-1* (APC3/Cdc27), *mat-2* (APC1/Tsg24), and *mat-3* (APC8/Cdc23). Phenotypic analysis of these temperature-sensitive APC/C mutants has suggested an absolute requirement for the

APC/C for metaphase-to-anaphase progression during germline meiosis and mitosis, but has not revealed significant somatic requirements. Null mutations in *emb-30/APC4* do cause some somatic defects, but due to perdurance of maternally provided gene product, these defects are apparent only in late-proliferating tissues such as the gonad, germline, male tail, and hermaphrodite vulva (FURUTA *et al.* 2000). Null mutations of other APC/C subunit genes have not yet been described.

Here we describe new alleles of the APC8 gene *mat-3*, including a likely null allele (*cs53*) and a hypomorphic viable allele (*ku233*) that reduces *mat-3* expression levels. Mutations in *lin-35/Rb* and other SynMuv B genes suppress *ku233* developmental defects and restore *mat-3* expression levels, suggesting that LIN-35/Rb and EFL-1/E2F normally repress *mat-3/APC8* transcription.

MATERIALS AND METHODS

General methods and strains: Standard methods were used for the handling and culturing of *C. elegans* (BRENNER 1974). Unless otherwise noted, experiments were performed at 20°. Mutations are described in RIDDLE *et al.* (1997) unless otherwise noted. Mutations used were:

- I: *dpy-5(e61)*, *lin-35(n745)*, *lin-53(n833)* (LU and HORVITZ 1998), *unc-13(e51)*.
- II: *dpl-1(n3643)* (CEOL and HORVITZ 2001), *fzr-1(ku298)* (FAY *et al.* 2002), *lin-8(n111)*, *hDf35* (KITAGAWA *et al.* 2002), *mIn1* (EDGLEY and RIDDLE 2001), *unc-4(e120)*.
- III: *daf-7(e1372)*, *dpy-1(e1)*, *lin-36(n766)*, *mat-3(ax68)* (GOLDEN *et al.* 2000), *ruls32 [unc-119(+)] pie-1::GFP::H2B* (PRAITIS *et al.* 1999), *unc-45(e286)*, *wcDf1* (TERNS *et al.* 1997).
- IV: *let-60(n1046gf)*.
- V: *efl-1(n3318)* (CEOL and HORVITZ 2001), *him-5(e1490)*.
- X: *lin-15(n309)*, *unc-1(e538)*.

Isolation of *mat-3* alleles: *ku233* was identified as an egg-laying defective mutant after gamma-irradiation (2400 rad) of strain MH620 [*lin-45(ku112) dpy-20(e1282)*] (M. SUNDARAM and M. HAN, unpublished results). Mapping experiments indicated that *ku233* maps very close and likely to the left of *unc-45* on chromosome III. Of 722 *ku233* homozygotes segregating from *ku233/unc-45* mothers, none were *unc-45/+*. Of 62 *ku233* not *daf-7* recombinants segregating from *ku233 daf-7/unc-45* mothers, none were *unc-45/+*. *ku233* was outcrossed with N2 six times to generate strain UP63, on which all phenotypic analyses were performed.

cs53 and *cs54* were isolated in a noncomplementation screen. *him-5* males were mutagenized with 50 mM EMS (BRENNER 1974) and crossed to *mat-3(ku233) daf-7; unc-1* hermaphrodites. Approximately 3500 non-Unc cross-progeny were screened for egg-laying defective (Egl) or protruding vulva phenotypes. Both *cs53* and *cs54* were outcrossed twice and balanced over *unc-45* to generate strains UP666 and UP668 on which all phenotypic analyses were performed.

Molecular analysis and rescue of *mat-3*: Genomic rescue fragments were generated by long-range PCR using Expand Long Template DNA polymerase (Roche Behringer). Primers oJD1 (GCCACGTGACTCTGCTGGAACCAA) and oDG43 (GGGAGGATAATCGACAAGGGG) and primers oDG55 (CCCCGCTGCTACTTCTCTG) and oDG43 were used to generate rescuing fragments PCR.JD1 and PCR.JD2, respectively. Primers oJD1 and oDG8 (CCGGGTGCGTAAAGGCTATTTC) were used to generate nonrescuing fragment PCR.JD3. To express cDNAs

TABLE 1
Genetic and phenotypic analyses of *mat-3* mutants

<i>mat-3</i> genotype	Phenotype			(n)	% abnormal vulva (n)
	Lethal (%)	Egl (%)	Sterile (%)		
<i>ku233</i> 15°	0	56	29	(99)	ND
<i>ku233</i> 20°	0	61	26	(99)	85 (186)
<i>ku233</i> 25°	0	11	0	(98)	61 (109)
<i>ku233/+</i> ^a	0	0	<1	(416)	ND
<i>ku233/wcDf1</i> ^b	<1	14	86	(37)	ND
<i>ku233/ax68</i> ^c 25°	1	49	33	(85)	ND
<i>ku233/cs53</i> ^d	0	6	94	(134)	ND
<i>ku233/cs54</i> ^d	0	7	93	(85)	ND
<i>cs53</i> ^e 25°	<2	NA	100	(320) ^e	100 (28) ^e
<i>cs53/wcDf1</i> ^f	<1	NA	100	(Many)	100 (16)
<i>cs54</i> ^g 25°	<2	NA	100	(235) ^g	100 (15) ^g
<i>cs54/wcDf1</i> ^f	<1	NA	100	(Many)	100 (19)

NA, not applicable; ND, not determined.

^a *ku233* was linked to *dpy-1*.

^b Animals were obtained as unmarked self-progeny from *ku233 daf-7/wcDf1 dpy-1* mothers.

^c Animals were obtained as non-Dpy progeny from a cross between *ax68; him-5* males and *ku233 dpy-1* hermaphrodites.

^d Animals were obtained as non-Dpy progeny from a cross between *cs53/+* or *cs54/+* males and *ku233 dpy-1* hermaphrodites. Approximately half of the progeny were wild type and inferred to be *+/ku233*.

^e *cs53/unc-45* mothers segregated 2% dead embryos and 22% Unc and 24% sterile progeny ($n = 320$), close to the expected Mendelian ratio if *cs53* were fully viable but sterile. Of the non-Unc progeny, 28/76 had abnormal vulvae, close to the expected fraction of *cs53* homozygotes.

^f Animals were obtained as unmarked progeny from a cross between *cs53 daf-7/unc-45* or *cs54 daf-7/unc-45* males and *unc-45 daf-7/wcDf1 dpy-1* hermaphrodites.

^g *cs54/unc-45* mothers segregated 2% dead embryos and 25% Unc and 29% sterile progeny ($n = 235$), close to the expected Mendelian ratio if *cs54* were fully viable but sterile. Of the non-Unc progeny, 15/46 had abnormal vulvae, close to the expected fraction of *cs54* homozygotes.

under the control of the *eft-3* promoter, *eft-3* promoter elements from TR#428 (MITROVICH and ANDERSON 2000) were cloned as a *SphI-XbaI* fragment into pPD49.26 (kindly provided by A. Fire) to generate pRH40. The full-length *mat-3* cDNA was amplified from clone yk459d5 with primers oJD12 (CTA GCTAGCAAAATGAACGTGAGTTTTTCAACT) and oJD13 (CGGGGTACCTCAAAAACGAGAAATCATCCTC) and cloned as an *NheI-KpnI* fragment into pRH40 to generate pJD10. PCR fragments (100 ng/ μ l) or pJD10 (10 ng/ μ l) were injected into *mat-3(ku233)* animals along with 100 ng/ μ l of the *rol-6^D* transformation marker pRF4 (MELLO *et al.* 1991). pRF4 alone had no effect on the *mat-3(ku233)* phenotype (data not shown).

To identify the *ku233* lesion, we PCR amplified and sequenced the *mat-3* genomic region between primers oDG55 and oDG43 from *ku233* mutant worms. The 2-bp changes found (Figure 2) are not present in the parental MH620 strain. To identify the *cs53* and *cs54* lesions we PCR amplified and sequenced all exons and exon/intron boundaries from mutant worms. *cs53* changes codon 274 (TGG, tryptophan) to TGA (stop). *cs54* changes the intron 7 splice donor from GT to AT.

Phenotypic characterization of *mat-3* mutants: General characterization of vulval development as normal *vs.* abnormal was based on differential interference contrast (DIC) observations of mid-L4 stage hermaphrodites. Vulval development was scored as normal if the vulval invagination was symmetric and contained 22 nuclei and abnormal if the vulval invagination

was asymmetric or contained <22 nuclei. Vulval cell divisions in wild-type, *mat-3(ku233)*, and *lin-35(n745)* mutants were also followed by DIC microscopy. To assess the length of mitosis in P_{n.p} or P_{n.px} cells, we recorded the time intervals between the completion of nucleolar breakdown, the appearance and disappearance of metaphase chromosomes, and the appearance of daughter nuclei. Only P_{5.p}–P_{7.p} (or their descendants) were followed. 4',6-Diamidino-2-phenylindole (DAPI) staining was performed by incubating L4 or adult-stage hermaphrodites in 200 mg/ml DAPI in ethanol for 30 min at room temperature.

RNAi experiments: RNAi was performed by microinjection essentially as described (FIRE *et al.* 1998). DNA templates were generated by PCR of cDNA clones yk434b7 (*cki-1*), yk131f10 (*fzr-1*), yk435e2 (*fzy-1*), yk117a4 (*lin-15A*), yk62g9 (*lin-15B*), yk13c4 (*lin-35*), pRH18 (*lin-36*), and yk143c11 (*lin-53*). Double-strand RNAs (dsRNAs) were prepared by *in vitro* transcription with T3 and T7 RNA polymerases [Ambion (Austin, TX) Megascript kit]. The effectiveness of dsRNA for each SynMuv gene was verified by testing for the ability to elicit a SynMuv phenotype in an appropriate genetic background [*lin-15A(n767)* or *lin-36(n766)*]. For all experiments, multiple adult hermaphrodites were injected with dsRNA and F₁ progeny laid >3 hr postinjection were scored.

Real-time PCR: Synchronized L1 larvae were obtained by hypochlorite treatment to select for embryos and subsequent culture in M9 buffer for 24–36 hr. L1 larvae were distributed

onto plates with food and allowed to grow for 32 hr, at which point most animals were at the mid-L3 stage. Larvae were then collected and RNA extracted using TRIZOL reagent (GIBCO-BRL, Gaithersburg, MD). A total of 650–1200 ng of total RNA from each strain was reverse transcribed using oligo-dT primer [Invitrogen (San Diego) Superscript First Strand Synthesis System for RT-PCR]. A total of 120–230 ng of first-strand cDNA was then used as template for real-time PCR using Taqman Universal PCR master mix (Applied Biosystems, Foster City, CA), probes labeled with the 5' reporter dye FAM and 3' quencher dye TAMRA, and a Perkin-Elmer (Norwalk, CT) ABI 7700 machine. Primers for *mat-3* were oJD16 (CGACTTGCGT TGATTCAACAG) and oJD19 (CCGCGCAAGTTGGTATCTT). Probe for *mat-3* was CGCCAGCCGGACAATACCGTG. Primers for reference mRNA *mek-2* were oJD23 (TGATTGATTTCGATG GCCAACT) and oJD24 (CAGGCACTGGATATCGTCCAA). Probe for *mek-2* was TTATATGGCGCCCGAACGACTCACA. *mek-2* levels were comparable across different samples with similar RNA inputs, indicating that the genotypes tested do not significantly alter *mek-2* expression (data not shown). Standard curves for *mat-3* and *mek-2* were generated using known concentrations of the cDNA-containing plasmids pJD10.2 and pMS73. Sequence Detector software 1.9.1 (Applied Biosystems) was used to calculate the copy numbers of *mat-3* and *mek-2* cDNAs.

RESULTS

Isolation of *mat-3* alleles: *mat-3(ku233)* was identified in a genetic screen for Egl mutants (MATERIALS AND METHODS). *mat-3(ku233)* homozygotes are viable and show incompletely penetrant Egl and sterile phenotypes. Both phenotypes are cold sensitive, being more highly penetrant at 15° or 20° than at 25° (Table 1). *ku233* appears to be a weak hypomorphic allele since the Egl and sterile phenotypes are recessive and sterility becomes more severe when *ku233* is placed *in trans* to *wcDf1* (a deficiency that removes the *mat-3* region; TERNS *et al.* 1997) or to other *mat-3* alleles (Table 1; see below). The *ku233* Egl and sterile phenotypes are rescued by introduction of a genomic transgene containing the *mat-3* operon as well as by ubiquitous expression of a *mat-3* cDNA construct (Figure 2A). We did not find any lesion within the *mat-3* coding region in *ku233* mutants; however, we did identify two adjacent base-pair changes ~400 bp upstream of the *mat-3* operon (Figure 2). These lesions affect a 16-bp potential *cis*-regulatory element conserved between *C. elegans* and the related species *C. briggsae* (Figure 2B). Real-time PCR experiments showed that *ku233* mutants have 5- to 10-fold lower levels of *mat-3* mRNA compared to wild type (WT; Table 2). Thus *ku233* mutants are likely to have reduced expression levels of an otherwise normal MAT-3 protein.

MAT-3 is a tetratricopeptide (TPR) repeat-containing protein orthologous to *Saccharomyces cerevisiae* Cdc23p and mammalian APC8 (DAVIS *et al.* 2002) and would be expected to be an essential subunit of the APC/C. All previously described *mat-3* alleles are temperature-sensitive embryonic lethals and cause few or no defects in postembryonic somatic development (GOLDEN *et al.* 2000; RAPPLEYE *et al.* 2002). A noncomplementation

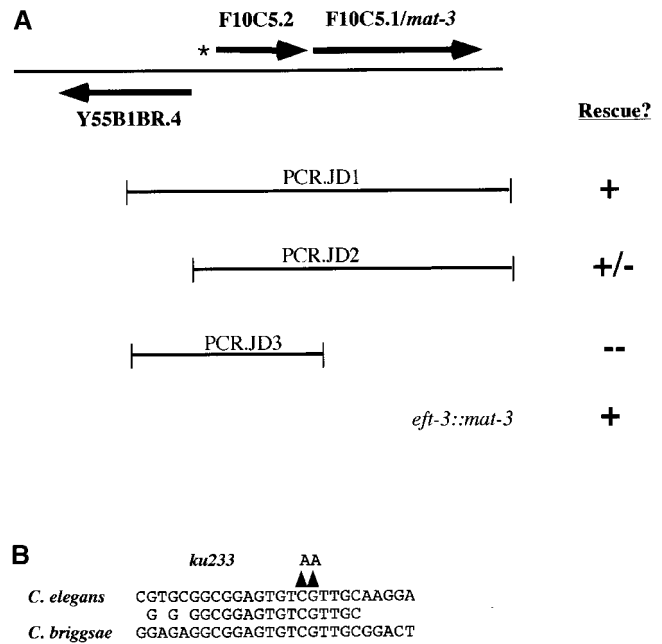


FIGURE 2.—The *mat-3(ku233)* lesion affects a conserved element upstream of the *mat-3* operon. (A) *mat-3* rescue constructs. F10C5.2 and *mat-3*/F10C5.1 appear to be part of an operon (DAVIS *et al.* 2002). Another predicted gene, Y55B1BR.4, is located close by on the opposite strand. *ku233* mutants contain 2-bp substitutions ~450 bp upstream of the F10C5.2 gene (asterisk). *ku233* Egl and sterile defects were rescued by PCR.JD1 and PCR.JD2, long-range PCR products containing the *mat-3* gene, and by pJD10, a plasmid containing the *mat-3* cDNA ubiquitously expressed under the control of the *eft-3* promoter (see MATERIALS AND METHODS). The percentage of fertile, egg-laying competent hermaphrodites was restored from <15% in *ku233* controls to >90% in transgenic animals. (B) Alignment of the *ku233* mutant regions between *C. elegans* and *C. briggsae*. TRANSFAC analysis (MATYS *et al.* 2003) did not detect any known transcription factor binding sites in this sequence.

screen with *ku233* (MATERIALS AND METHODS) identified two strong nonconditional *mat-3* alleles, *cs53* and *cs54*. Homozygotes for either allele are viable but have a variety of developmental defects and are completely sterile (Table 1). *cs53* is a nonsense mutation predicted to truncate the MAT-3 protein after the first TPR repeat (MATERIALS AND METHODS). *cs54* affects a splice donor site (MATERIALS AND METHODS). Both the molecular lesion and deficiency experiments (Table 1) suggest that *cs53* is likely null.

Phenotypic characterization of *mat-3* mutants: Embryonic and early larval development appear normal even in the strongest *mat-3* mutants, apparently due to perdurance of maternally provided gene product. However, all three *mat-3* alleles cause developmental defects in late-proliferating tissues such as the gonad, germline, male tail, and hermaphrodite vulva (Figures 3 and 4).

mat-3(cs53) animals have the most severe defects. At the L4 stage, *cs53* mutant germlines contain an increased number of mitotic germ nuclei arrested at metaphase as

TABLE 2
lin-35/Rb and *dpl-1*/DP mutations restore
mat-3 mRNA levels in *ku233* mutants

Genotype ^a	Normalized <i>mat-3</i> expression \pm SD ^b	Range of means ^c	No. of experiments
WT	1.0 \pm 0.23	1.0	9
<i>ku233</i>	0.13 \pm 0.02	0.08–0.2	6
<i>ku233; fzr-1</i>	0.32 \pm 0.07	0.25–0.41	3
<i>ku233; lin-35</i>	1.51 \pm 0.49	0.80–2.12	5
<i>ku233; dpl-1</i>	0.68 \pm 0.06	0.38–0.91	5
<i>ku233; lin-36</i>	0.23 \pm 0.04	0.12–0.31	3
<i>lin-35</i>	1.64 \pm 0.12	1.47–1.75	3
<i>dpl-1</i>	2.35 \pm 0.42	2.09–2.54	3
<i>lin-36</i>	2.30 \pm 0.18	1.93–2.55	3

^a Alleles used were *fzr-1(ku298)*, *lin-35(n765)*, *dpl-1(n3643)*, and *lin-36(n766)*. *lin-35* was linked to *unc-13*.

^b *mat-3* expression levels were assessed by real-time PCR in relation to that of the reference mRNA *mek-2* (MATERIALS AND METHODS). All PCR amplifications within an experiment were done in duplicate and relative *mat-3* levels were calculated as the ratio of the *mat-3* and *mek-2* means and then normalized by setting wild-type levels to 1.0. Numbers shown are mean \pm standard deviation (SD) for normalized values across all experiments.

^c The range of means across different experiments is indicated.

assessed by DAPI staining (approximately fourfold greater than that of wild type; Figure 3B). By adulthood, mutant germlines appear to disintegrate such that no germ nuclei are present in the distal part of the gonad (Figure 3F) and no sperm or oocytes are ever formed. Males lack rays and spicules (data not shown), and hermaphrodites show severely reduced numbers of vulval nuclei (Figure 4F). These defects are similar to those reported for null mutations in *emb-30/APC4* (FURUTA *et al.* 2000) and are consistent with a requirement for the APC/C during somatic and germline mitosis.

mat-3(ku233) animals have weaker defects and can be propagated as a homozygous strain. *ku233* hermaphrodites do not have obvious defects in germline mitosis (Figure 3D) and most animals produce morphologically normal sperm and oocytes and give rise to live progeny. However, some animals have mislocalized sperm within the uterine cavity or distal gonad (data not shown) and/or accumulate oocytes with abnormal chromosome morphologies (Figure 3H). Embryonic and early larval development is apparently normal, but most *ku233; him-5* males have abnormal spicules (78%, $n = 27$) and most *ku233* hermaphrodites have abnormal vulvae (85%, $n = 186$; Figure 4, B, D, H, and I). The development of these sex-specific structures therefore seems particularly sensitive to the reduction in *mat-3* expression.

By observing the vulval lineages (see Figure 1) in *ku233* mutants, we found that the vulval precursor cells P3.p–P8.p appear morphologically normal and divide

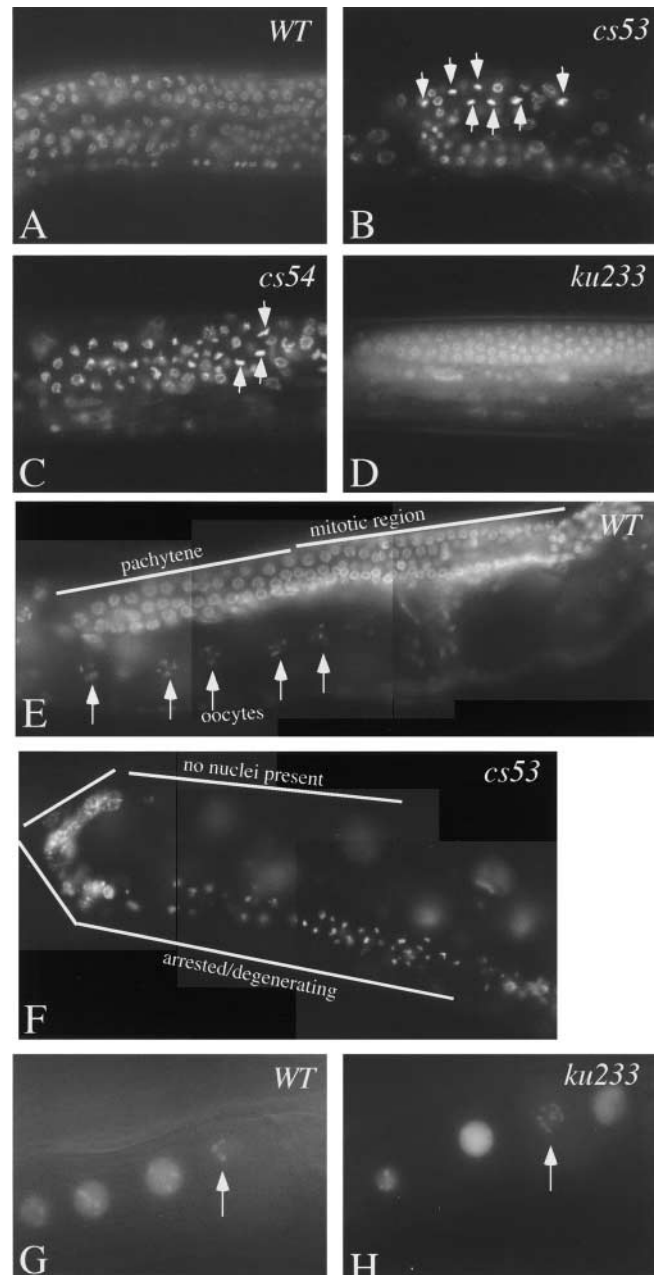


FIGURE 3.—Germline phenotypes of *mat-3* mutants. (A–D) The average number of metaphase nuclei (arrows) per gonad arm was assessed in DAPI-stained L4 hermaphrodites. (A) WT (1.8 ± 1.0 , $n = 20$). (B) *cs53* (7.2 ± 2.7). (C) *cs54* (not quantitated). (D) *ku233* (1.8 ± 1.4 , $n = 17$). (E and F) DAPI-stained adult hermaphrodites. (E) WT, showing normal mitotic and meiotic (pachytene) nuclei and mature oocytes (arrows). (F) *cs53*, showing deteriorated germline. (G and H) Adult hermaphrodites expressing the histone2B::GFP reporter *ruls32* (PRAITIS *et al.* 1999). (G) WT, with six bivalents visible in proximal oocyte (arrow). (H) *ku233*, with more than six bivalents visible in oocyte (arrow). The distal gonad (dorsal) is on the top in all images.

with a lengthened mitosis (see below) to generate morphologically normal Pn.px daughter cells. Some Pn.px cells occasionally fail to divide (Figure 4H), but most divide with a lengthened mitosis (see below) to generate

Pn.pxx daughters of variable nuclear size and positioning (Figure 4B). The last round of vulval divisions is highly abnormal and *Pn.pxxx* nuclei sometimes fail to resolve (Figure 4D). By the mid-L4 stage, the vulval invagination appears grossly disorganized (Figure 4I).

To characterize further the mitotic delays seen during vulval cell divisions, we compared the timing of mitotic progression in wild-type *vs.* *ku233* mutants (Table 3). In wild type, nucleolar breakdown is the first observable indication of mitotic entry. Within a few minutes of nucleolar breakdown, metaphase chromosomes become visible as two parallel lines and then persist for ~5 min before separating at anaphase and disappearing from

view. Approximately 5 min later, the daughter nuclei appear. In *ku233* mutants, nucleolar breakdown is followed closely by the appearance of metaphase chromosomes, which then persist for more than twice the normal time (Table 3). There is also a delay between the disappearance of the chromosomes following anaphase and the appearance of the daughter nuclei (Table 3). Thus *ku233* mutants appear to be defective at the metaphase-to-anaphase transition as well as in subsequent exit from mitosis.

***mat-3(ku233)* defects are mimicked by reducing *fzy-1* and are suppressed by reducing *fzr-1*:** Core APC/C components such as APC8 associate with different regulatory subunits, Fzy or Fzr, to regulate different steps of the cell cycle (see Introduction). The extended metaphase observed during *mat-3(ku233)* vulval development suggests a defect in APC/C-Fzy function. Consistent with this hypothesis, *fzy-1(RNAi)* caused *ku233*-like vulval defects (Table 4, Figure 4J). In contrast, the hypomorphic allele *fzr-1(ku298)* caused few vulval defects (Table 4). Surprisingly, both *fzr-1(ku298)* and *fzr-1(RNAi)* partly suppressed the *ku233* vulval defects (Table 4, Figure 4K). Real-time PCR experiments demonstrated that *fzr-1* slightly increases the level of *mat-3* mRNA (Table 2), but it is not clear if this modest effect is sufficient to explain the observed suppression. In other systems, APC/C-Fzr has been shown to target Fzy for proteasome-mediated destruction (HARPER *et al.* 2002; PETERS 2002). If *fzr-1* mutations elevate FZY-1 levels, this would be a potential alternative mechanism to explain how *fzr-1* suppresses *ku233*. These experiments demonstrate that APC/C-Fzr activity is largely intact in *ku233* mutants and that APC/C-Fzy is more sensitive than APC/C-Fzr to the reduction in *mat-3* expression.

***lin-35/Rb* and other synthetic multivulva mutations suppress *mat-3(ku233)* defects:** We discovered that certain class B SynMuv mutations are strong suppressors of *mat-3(ku233)* defects (Table 4, Figure 4L). We initially found that the Multivulva mutant *lin-15(n309)* efficiently suppresses *ku233* sterile, Egl, and vulval defects. *lin-15* is a complex locus containing two SynMuv genes, *lin-15A*

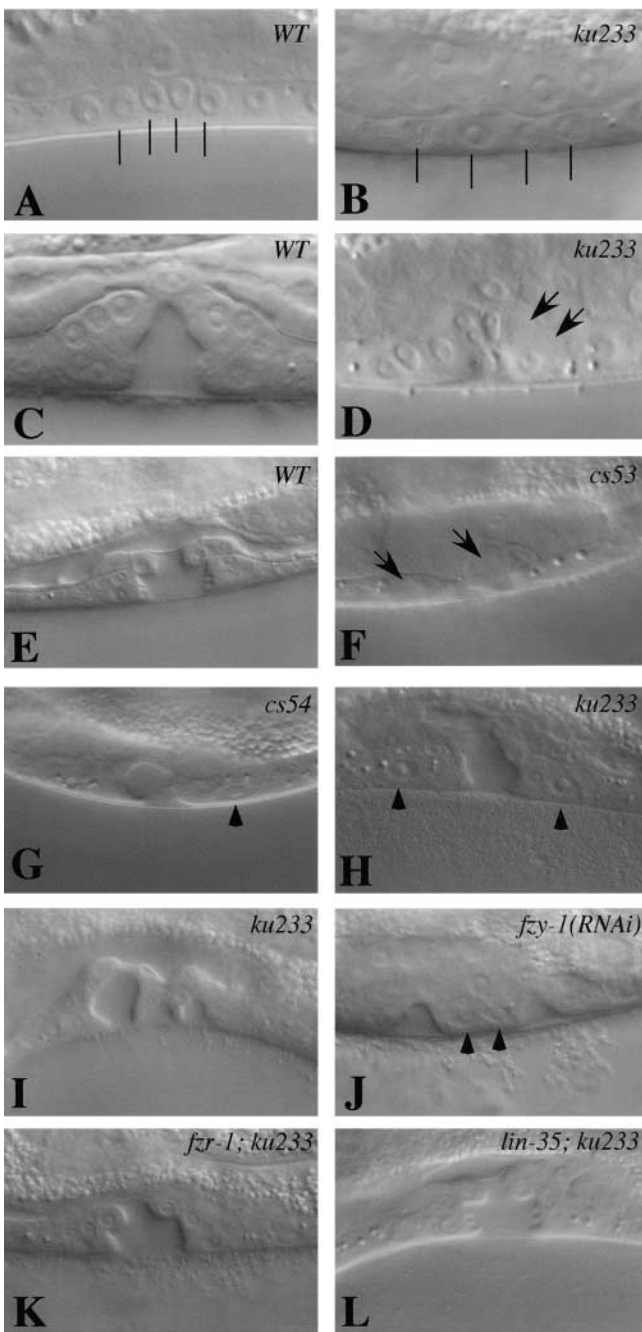


FIGURE 4.—Vulval defects of *mat-3* mutants and suppression by *fzr-1* and SynMuv mutations. (A) WT, late L3, with four equally sized P6.pxx nuclei (lines). (B) *ku233*, late L3, showing unequally sized P6.pxx nuclei (lines). (C) WT, early L4. (D) *ku233*, early L4, showing disorganized invagination and some unresolved cell divisions (arrows). (E) WT, mid-L4. (F) *cs53*, mid-L4, showing widespread unresolved cell divisions (arrows). (G) *cs54*, mid-L4, showing undivided P7.pp nucleus (arrowhead). (H) *ku233*, mid-L4, showing undivided P5.pp and P7.pp nuclei (arrowheads). (I) *ku233*, mid-L4, showing multiple disorganized invaginations. (J) *fzy-1(RNAi)*, mid-L4, showing multiple disorganized invaginations and undivided P6.px nuclei (arrowheads). (K) *fzr-1(ku298); ku233*, mid-L4, showing suppression of vulval defects (compare to E). (L) *lin-35(n745); ku233*, mid-L4, showing suppression of vulval defects (compare to E).

TABLE 3
mat-3(ku233) mutants have delays in mitotic progression

Genotype	Division	Average minutes \pm SD			n
		Prophase ^a	Metaphase/anaphase ^b	Telophase ^c	
WT	Pn.p-px	3.3 \pm 2.1	4.9 \pm 1.5	5.3 \pm 1.0	11
	Pn.px-pxx	2.8 \pm 1.6	5.6 \pm 1.5	5.2 \pm 1.5	5
<i>mat-3(ku233)</i>	Pn.p-px	3.7 \pm 0.6	17.7 \pm 1.5	13.3 \pm 1.5	3
	Pn.px-pxx	2.5 \pm 0.6	14.7 \pm 0.5	11.2 \pm 2.5	4
<i>lin-35(n745)</i>	Pn.p-px	ND	ND	ND	
	Pn.px-pxx	4.0 \pm 1.7	4.9 \pm 1.1	6.6 \pm 1.7	8

^a Time between complete nucleolar breakdown and start of metaphase. Actual start of prophase is likely several minutes earlier.

^b Time that aligned chromosomes were visible. Anaphase corresponds to <1 min in all genotypes.

^c Time between disappearance of separating chromosomes and appearance of daughter nuclei.

and *lin-15B* (CLARK *et al.* 1994; HUANG *et al.* 1994). Suppression by *lin-15(n309)* can be attributed to a loss of *lin-15B* activity since *lin-15B(RNAi)*, but not *lin-15A(RNAi)*, efficiently suppressed *ku233* vulval defects. A subset of other class B SynMuv mutations (but no class A SynMuv mutations) also suppresses *ku233* vulval defects (Table 4); these include *lin-35/Rb* and *efl-1/E2F* as well as *dpl-1/DP* (an E2F dimerization partner; CEOL and HORVITZ 2001). A dominant-negative allele of *lin-53/RbAp48* (an Rb-binding protein; LU and HORVITZ 1998) suppresses *ku233* defects but *lin-53(RNAi)* does not (Table 4), suggesting that suppression is not due to loss of *lin-53/RbAp48* function. Notably, although the class B synMuv gene *lin-36* acts with *lin-35/Rb* to inhibit G₁-to-S progression (BOXEM and VAN DEN HEUVEL 2002; FAY *et al.* 2002), mutations in *lin-36* do not suppress *ku233* (Table 4). Reduction of the G₁/S regulator *cki-1* (a cyclin kinase inhibitor; HONG *et al.* 1998) also does not suppress *ku233* (Table 4). The *let-60 ras* gain-of-function allele *n1046* also does not suppress *ku233* (Table 4). Therefore, suppression of *ku233* is not a general property of mutations that bypass G₁ arrest or that increase vulval fate induction or Ras signaling, but is instead a specific property of a subset of SynMuv B genes.

Suppression appears specific to the *mat-3(ku233)* allele since *lin-15(n309)* does not suppress the vulval or sterile defects of *mat-3(cs53)* or *mat-3(cs54)* mutants (Table 4); *lin-15(n309)*, *lin-35(n765)*, or *lin-35(RNAi)* do not suppress the embryonic lethality of *mat-3(ax68)* temperature-sensitive mutants (data not shown); and *lin-35(RNAi)* does not suppress the embryonic lethality of *mat-3(or180)* temperature-sensitive mutants (data not shown). Therefore, SynMuv mutations do not bypass the requirement for *mat-3*. Instead, SynMuv mutations may compensate for reduced *mat-3* activity in *ku233* mutants or may restore *mat-3* activity to more wild-type levels.

***lin-35/Rb* and *dpl-1/DP* mutations restore *mat-3* mRNA levels in *ku233* mutants:** Since LIN-35/Rb and other

SynMuv gene products are likely transcriptional regulators, one possible model to explain our findings is that these proteins normally repress *mat-3* gene expression. In this case, mutations in SynMuv B genes would suppress *mat-3(ku233)* by increasing *mat-3* expression levels. In support of this model, real-time PCR revealed that both *lin-35/Rb* and *dpl-1/DP* mutations increase *mat-3* mRNA levels in *mat-3(ku233)* mutants to near wild-type or greater than wild-type levels (Table 2). In contrast, a *lin-36* mutation that does not suppress *mat-3(ku233)* defects does not significantly increase *mat-3* mRNA expression (Table 2). Thus changes in *mat-3* expression levels correlate well with phenotypic suppression.

lin-35/Rb and *dpl-1/DP* mutations slightly increase *mat-3* gene expression in a *mat-3(+)* background, but the effect is not as dramatic as that seen in the *ku233* background and is similar to that caused by a *lin-36* mutation (Table 2). Thus, as for many other effects of SynMuv genes, the repressive effects of *lin-35/Rb* and *dpl-1/DP* on *mat-3* are detected only in a sensitized genetic background—in this case in the context of the *ku233* mutation that reduces *mat-3* expression. We propose that a positive regulatory element affected by the *ku233* lesion normally counteracts the repressive influence of *lin-35/Rb*, *dpl-1/DP*, *efl-1/E2F*, and other SynMuv B gene products.

DISCUSSION

We have shown that *lin-35/Rb* and a subset of other SynMuv B genes (*efl-1/E2F*, *dpl-1/DP*, and *lin-15B*) negatively regulate *mat-3/APC8* expression. Reducing the activity of these SynMuv B genes can suppress mitotic defects caused by inadequate *mat-3*. Although our data do not distinguish between direct and indirect effects, it is possible that Rb/E2F complexes directly repress *mat-3* transcription. This study shows that Rb and E2F can affect mitotic progression *in vivo* and further ex-

TABLE 4
Suppression of *mat-3(ku233)* defects by *fzr-1*
and SynMuv B mutations

Genotype ^a		SynMuv class	% abnormal vulva (n)
<i>mat-3</i>	Other		
+	+	—	0 (many)
+	<i>fzy-1(RNAi)</i> 25°	—	41 (22)
+	<i>fzr-1(ku298)</i>	—	10 (21)
<i>ku233</i>	+	—	85 (186)
<i>ku233</i>	<i>fzy-1(RNAi)</i>	—	80 (51)
<i>ku233</i>	<i>fzr-1(ku298)</i>	—	25 (16)
<i>ku233</i>	<i>fzr-1(RNAi)</i>	—	26 (47)
<i>ku233</i>	<i>lin-15(n309)</i>	AB	0 (12)
<i>ku233</i>	<i>lin-15A(RNAi)</i>	A	85 (68)
<i>ku233</i>	<i>lin-15B(RNAi)</i>	B	4 (53)
<i>ku233</i>	<i>lin-8(n111)</i>	A	77 (22)
<i>ku233</i>	<i>lin-35(RNAi)</i>	B	14 (84)
<i>ku233</i>	<i>lin-35(n745)</i>	B	0 (16)
<i>ku233</i>	<i>lin-36(RNAi)</i>	B	84 (149)
<i>ku233</i>	<i>lin-36(n766)</i>	B	88 (17)
<i>ku233</i>	<i>lin-53(RNAi)</i>	B	79 (38)
<i>ku233</i>	<i>lin-53(n833)</i>	B	0 (31)
<i>ku233</i>	<i>dpl-1(n3643)</i>	B	0 (35)
<i>ku233</i>	<i>eft-1(RNAi)</i>	B	28 (64)
<i>ku233</i>	<i>cki-1(RNAi)</i>	—	100 (28)
<i>ku233</i>	<i>let-60(n1046gf)</i>	—	94 (18)
<i>cs53</i>	<i>lin-15(n309)</i> 25°	AB	100 (9) ^b
<i>cs54</i>	<i>lin-15(n309)</i> 25°	AB	100 (24) ^b

^a *fzr-1* was linked to marker *unc-4*. *lin-35* was linked to marker *unc-13*. Note that *lin-53(n833)* is a dominant-negative allele and behaves differently from *lin-53(RNAi)* (see text). The effectiveness of RNAi against each SynMuv gene was verified by testing for the ability to elicit a SynMuv phenotype in an appropriate genetic background [*lin-15A(n767)* or *lin-36(n766)*]. RNAi against *fzy-1*, *lin-53*, *eft-1*, or *cki-1* caused embryonic lethality, so only escapers could be scored. RNAi against *fzr-1* caused some animals to lack a gonad and vulva; these were excluded from the data set.

^b Experiments were performed at 25°. Of the non-Unc animals from *cs53/unc-45*; *n309* mothers, 9/25 had abnormal vulval nuclei, close to the expected fraction of *cs53* homozygotes. Of the non-Unc animals from *cs54/unc-45*; *n309* mothers, 24/81 had abnormal vulval nuclei, close to the expected fraction of *cs54* homozygotes. All fertile animals in the stocks gave both Unc and sterile progeny, indicating that *lin-15* does not suppress the sterility of *mat-3(cs53)* or *mat-3(cs54)*.

pands the known roles of these proteins outside of G₁/S regulation.

Transcriptional regulation of *mat-3*: The *mat-3(ku233)* lesion disrupts a conserved sequence element important for *mat-3* expression. It appears that this positive element normally counteracts the repressive influence of *lin-35/Rb*, *dpl-1/DP*, *eft-1/E2F*, and other SynMuv B gene products. In *ku233* mutants that lack the positive element, *mat-3* expression is strongly repressed by SynMuv proteins. Removing the SynMuv proteins restores *mat-3* expression and suppresses *ku233* mutant defects. In wild-type animals where the positive element is intact,

SynMuv proteins appear to have a smaller (but still detectable) impact on *mat-3* expression, possibly because they are inhibited or antagonized by factors binding to the positive element. We do not know what factors normally bind to the positive element. TRANSFAC analysis (MATYS *et al.* 2003) did not detect any known transcription factor binding sites in this sequence.

Our data do not distinguish between direct and indirect effects of the SynMuv proteins. It is possible that Rb/E2F complexes directly repress *mat-3* transcription since there is one perfect E2F consensus binding site (GCGCGAAAA) ~130 bp upstream of the *mat-3* operon, and the TRANSFAC program (MATYS *et al.* 2003) predicts >40 other potential E2F binding sites within the noncoding regions of the genomic *mat-3* rescue fragment PCR.JD2 (data not shown). Alternatively, it is possible that Rb/E2F regulate other factors that ultimately impact on *mat-3* expression. We are confident that phenotypic suppression of *ku233* is a result and not a cause of the elevated *mat-3* mRNA levels since we have identified a novel suppressor of *ku233* that has no detectable effect on *mat-3* mRNA levels (our unpublished data). Further studies will be needed to determine if Rb/E2F complexes act directly or indirectly on the *mat-3* gene promoter and whether regulation of *mat-3* varies in different stages of the cell cycle.

Redundant functions of *lin-35/Rb*: *lin-35* appears to be the only Rb-related gene in *C. elegans* (LU and HORVITZ 1998), so it is somewhat surprising that *lin-35* mutants have very few defects. Multiple studies have now shown that *lin-35* functions redundantly with other genes to control a variety of different processes. *lin-35* functions redundantly with cyclin kinase inhibitors and *fzr-1* to inhibit G₁-to-S progression (BOXEM and VAN DEN HEUVEL 2001; FAY *et al.* 2002), with SynMuv A genes to inhibit vulval fate induction (LU and HORVITZ 1998), and with *ubc-18* to promote proper pharyngeal development (FAY *et al.* 2003). The work described here raises the possibility that *lin-35* may also function redundantly with other unknown genes to regulate mitosis (see below).

***lin-35/Rb* acts with distinct subsets of partners to regulate different processes:** *lin-35/Rb* appears to act with different subsets of genes to regulate different processes. For example, *lin-35* acts with a set of more than a dozen other SynMuv B genes to inhibit vulval fate induction (THOMAS *et al.* 2003), but acts with only a subset of these SynMuv B genes to regulate G₁/S progression (BOXEM and VAN DEN HEUVEL 2002). We have shown that *lin-35* acts with a distinct subset of SynMuv B genes to regulate *mat-3*. Since Rb, E2F, and orthologs of some other SynMuv B gene products are known to form protein complexes that remodel chromatin and alter transcription (HARBOUR and DEAN 2000; STEVAUX and DYSON 2002), a reasonable model based on the genetic observations is that LIN-35/Rb participates in distinct protein complexes at different gene promoters. The presence of unique components in these different

complexes could target the complex to distinct promoters and/or could allow for specific regulation of the core complex (for example, by signaling pathways or cell-cycle factors). Screens for suppressors of *mat-3(ku233)* defects may identify additional gene products that act with *lin-35*/Rb to repress *mat-3*.

Potential mitotic requirements for *lin-35*/Rb: Our finding that *lin-35*/Rb represses *mat-3* expression is consistent with microarray and chromatin precipitation experiments in mammalian cells and in *Drosophila* showing that Rb/E2F regulate transcription of a variety of mitotic and spindle checkpoint genes (ISHIDA *et al.* 2001; MULLER *et al.* 2001; REN *et al.* 2002; DIMOVA *et al.* 2003). The functional significance of this regulation is not understood, but it is possible that by regulating the expression of mitotic genes such as *mat-3*/APC8, Rb/E2F could control the timing of mitotic progression during development and/or protect cells against chromosome damage or loss caused by inappropriate mitotic progression. We have not found evidence for altered mitotic timing in *lin-35*/Rb single mutants (Table 3). However, as has been found for its other roles, any mitotic or spindle checkpoint roles of *lin-35*/Rb may be redundant or detectable only under certain stressful conditions. It will be interesting to determine if any of the mutations that cause synthetic lethality with *lin-35* (FAY *et al.* 2002) result in mitotic dysregulation.

We are very grateful for the support of Min Han, in whose lab *ku233* was originally isolated. We also thank Craig McKinnon and Ben Williams for sharing *pat-4* map information and alleles, Yuji Kohara for cDNA clones, Phil Anderson, Andy Fire, and Robyn Howard for vectors, Farida Shaheen and the Center for Aids Research at the University of Pennsylvania for help with real-time PCR, Bruce Wightman and Chris Rocheleau for comments on the manuscript, and Andy Golden and members of our laboratory for helpful discussions and advice. Some strains were provided by the *Caenorhabditis* Genetics Center, which is supported by a grant from the National Center for Research Resources. This work was supported by a March of Dimes grant to M.S.

LITERATURE CITED

- BOXEM, M., and S. VAN DEN HEUVEL, 2001 *lin-35* Rb and *chi-1* Cip/Kip cooperate in developmental regulation of G1 progression in *C. elegans*. *Development* **128**: 4349–4359.
- BOXEM, M., and S. VAN DEN HEUVEL, 2002 *C. elegans* class B synthetic multivulva genes act in G1 regulation. *Curr. Biol.* **12**: 906–911.
- BRENNER, S., 1974 The genetics of *Caenorhabditis elegans*. *Genetics* **77**: 71–94.
- CEOL, C. J., and H. R. HORVITZ, 2001 *dpl-1* DP and *efl-1* E2F act with *lin-35* Rb to antagonize Ras signaling in *C. elegans* vulval development. *Mol. Cell* **7**: 461–473.
- CLARK, S. G., X. LU and H. R. HORVITZ, 1994 The *Caenorhabditis elegans* locus *lin-15*, a negative regulator of a tyrosine kinase signaling pathway, encodes two different proteins. *Genetics* **137**: 987–997.
- DAHIYA, A., S. WONG, S. GONZALO, M. GAVIN and D. C. DEAN, 2001 Linking the Rb and Polycomb pathways. *Mol. Cell* **8**: 557–568.
- DAVIS, E. S., L. WILLE, B. A. CHESTNUT, P. L. SADLER, D. C. SHAKES *et al.*, 2002 Multiple subunits of the *Caenorhabditis elegans* anaphase-promoting complex are required for chromosome segregation during meiosis I. *Genetics* **160**: 805–813.
- DAWSON, I. A., S. ROTH and S. ARTAVANIS-TSAKONAS, 1995 The *Drosophila* cell cycle gene *fizzy* is required for normal degradation of cyclins A and B during mitosis and has homology to the CDC20 gene of *Saccharomyces cerevisiae*. *J. Cell Biol.* **129**: 725–737.
- DEGREGORI, J., T. KOWALIK and J. R. NEVINS, 1995 Cellular targets for activation by the E2F1 transcription factor include DNA synthesis and G1/S-regulatory genes. *Mol. Cell Biol.* **15**: 4215–4224.
- DIMOVA, D. K., O. STEVAUX, M. V. FROLOV and N. J. DYSON, 2003 Cell cycle-dependent and cell cycle-independent control of transcription by the *Drosophila* E2F/RB pathway. *Genes Dev.* **17**: 2308–2320.
- EDGLEY, M. L., and D. L. RIDDLE, 2001 LG II balancer chromosomes in *Caenorhabditis elegans*: *mT1(II;III)* and the *mIn1* set of dominantly and recessively marked inversions. *Mol. Genet. Genomics* **266**: 385–395.
- FAY, D. S., S. KEENAN and M. HAN, 2002 *fzr-1* and *lin-35*/Rb function redundantly to control cell proliferation in *C. elegans* as revealed by a nonbiased synthetic screen. *Genes Dev.* **16**: 503–517.
- FAY, D. S., E. LARGE, M. HAN and M. DARLAND, 2003 *lin-35*/Rb and *ubc-18*, an E2 ubiquitin-conjugating enzyme, function redundantly to control pharyngeal morphogenesis in *C. elegans*. *Development* **130**: 3319–3330.
- FERGUSON, E. L., and H. R. HORVITZ, 1989 The multivulva phenotype of certain *Caenorhabditis elegans* mutants results from defects in two functionally redundant pathways. *Genetics* **123**: 109–121.
- FIRE, A., S. XU, M. K. MONTGOMERY, S. A. KOSTAS, S. E. DRIVER *et al.*, 1998 Potent and specific genetic interference by double-stranded RNA in *Caenorhabditis elegans*. *Nature* **391**: 806–811.
- FURUTA, T., S. TUCK, J. KIRCHNER, B. KOCH, R. AUTY *et al.*, 2000 EMB-30: an APC4 homologue required for metaphase-to-anaphase transitions during meiosis and mitosis in *Caenorhabditis elegans*. *Mol. Biol. Cell* **11**: 1401–1419.
- GOLDEN, A., P. L. SADLER, M. R. WALLENFANG, J. M. SCHUMACHER, D. R. HAMILL *et al.*, 2000 Metaphase to anaphase (*mat*) transition defective mutants in *Caenorhabditis elegans*. *J. Cell Biol.* **151**: 1469–1482.
- HARBOUR, J. W., and D. C. DEAN, 2000 The Rb/E2F pathway: expanding roles and emerging paradigms. *Genes Dev.* **14**: 2393–2409.
- HARPER, J. W., J. L. BURTON and M. J. SOLOMON, 2002 The anaphase-promoting complex: it's not just for mitosis any more. *Genes Dev.* **16**: 2179–2206.
- HONG, Y., R. ROY and V. AMBROS, 1998 Developmental regulation of a cyclin-dependent kinase inhibitor controls postembryonic cell cycle progression in *Caenorhabditis elegans*. *Development* **125**: 3585–3597.
- HUANG, L. S., P. TZOU and P. W. STERNBERG, 1994 The *lin-15* locus encodes two negative regulators of *Caenorhabditis elegans* vulval development. *Mol. Biol. Cell* **5**: 395–411.
- ISHIDA, S., E. HUANG, H. ZUZAN, R. SPANG, G. LEONE *et al.*, 2001 Role for E2F in control of both DNA replication and mitotic functions as revealed from DNA microarray analysis. *Mol. Cell Biol.* **21**: 4684–4699.
- KITAGAWA, R., E. LAW, L. TANG and A. M. ROSE, 2002 The Cdc20 homolog, FZY-1, and its interacting protein, IFY-1, are required for proper chromosome segregation in *Caenorhabditis elegans*. *Curr. Biol.* **12**: 2118–2123.
- LU, X., and H. R. HORVITZ, 1998 *lin-35* and *lin-53*, two genes that antagonize a *C. elegans* Ras pathway, encode proteins similar to Rb and its binding protein RbAp48. *Cell* **95**: 981–991.
- LUKAS, C., C. S. SORENSON, E. KRAMER, E. SANTONI-RIGIU, C. LINDENEG *et al.*, 1999 Accumulation of cyclin B1 requires E2F and cyclin-A-dependent rearrangement of the anaphase-promoting complex. *Nature* **401**: 815–818.
- MATYS, V., E. FRICKE, R. GEFFERS, E. GOSSLING, M. HAUBROCK *et al.*, 2003 TRANSFAC: transcriptional regulation, from patterns to profiles. *Nucleic Acids Res.* **31**: 374–378.
- MELLO, C. C., J. M. KRAMER, D. STINGHCOMB and V. AMBROS, 1991 Efficient gene transfer in *C. elegans* after microinjection of DNA into germline cytoplasm: extrachromosomal maintenance and integration of transforming sequences. *EMBO J.* **10**: 3959–3970.
- MITROVICH, Q. M., and P. ANDERSON, 2000 Unproductively spliced ribosomal protein mRNAs are natural targets of mRNA surveillance in *C. elegans*. *Genes Dev.* **14**: 2173–2184.
- MULLER, H., A. BRACKEN, R. VERNELL, M. C. MORONI, F. CHRISTIANS *et al.*, 2001 E2Fs regulate the expression of genes involved in

- differentiation, development, proliferation, and apoptosis. *Genes Dev.* **15**: 267–285.
- OHTANI, K., J. DEGREGORI and J. R. NEVINS, 1995 Regulation of the cyclin E gene by transcription factor E2F1. *Proc. Natl. Acad. Sci. USA* **92**: 12146–12150.
- PETERS, J. M., 2002 The anaphase-promoting complex: proteolysis in mitosis and beyond. *Mol. Cell* **9**: 931–943.
- PRAITIS, V., E. CASEY, D. COLLAR and J. AUSTIN, 1999 Creation of low-copy integrated transgenic lines in *Caenorhabditis elegans*. *Genetics* **157**: 1217–1226.
- RAPPELLE, C. A., A. TAGAWA, R. LYCZAK, B. BOWERMAN and R. V. AROIAN, 2002 The anaphase promoting complex and separin are required for embryonic anterior-posterior axis formation. *Dev. Cell* **2**: 195–206.
- REN, B., H. CAM, Y. TAKAHASHI, T. VOLKERT, J. TERRAGNI *et al.*, 2002 E2F integrates cell cycle progression with DNA repair, replication, and G(2)/M checkpoints. *Genes Dev.* **16**: 245–256.
- RIDDLE, D. L., T. BLUMENTAL, B. J. MEYER and J. R. PRIESS (Editors), 1997 *C. elegans II*. Cold Spring Harbor Laboratory Press, Plainview, NY.
- SCHULZE, A., K. ZERFASS, D. SPITKOVSKY, S. MIDDENDORP, J. BERGES *et al.*, 1995 Cell cycle regulation of the cyclin A gene promoter is mediated by a variant E2F site. *Proc. Natl. Acad. Sci. USA* **92**: 11264–11268.
- SHAKES, D. C., P. L. SADLER, J. M. SCHUMACHER, M. ABDOLRASULNIA and A. GOLDEN, 2003 Developmental defects observed in hypomorphic anaphase-promoting complex mutants are linked to cell cycle abnormalities. *Development* **130**: 1605–1620.
- SIGRIST, S. J., and C. F. LEHNER, 1997 *Drosophila* fizzy-related down-regulates mitotic cyclins and is required for cell proliferation arrest and entry into endocycles. *Cell* **90**: 671–681.
- SIGRIST, S., H. JACOBS, R. STRATMANN and C. F. LEHNER, 1995 Exit from mitosis is regulated by *Drosophila* fizzy and the sequential destruction of cyclins A, B and B3. *EMBO J.* **14**: 4827–4838.
- STEVAUX, O., and N. J. DYSON, 2002 A revised picture of the E2F transcriptional network and RB function. *Curr. Opin. Cell Biol.* **14**: 684–691.
- SULSTON, J. E., and H. R. HORVITZ, 1977 Post-embryonic cell lineages of the nematode *Caenorhabditis elegans*. *Dev. Biol.* **56**: 110–156.
- SULSTON, J. E., and J. G. WHITE, 1980 Regulation and cell autonomy during postembryonic development of *Caenorhabditis elegans*. *Dev. Biol.* **78**: 577–597.
- TERNS, R. M., P. KROLL-CONNOR, J. ZHU, S. CHUNG and J. H. ROTHMAN, 1997 A deficiency screen for zygotic loci required for establishment and patterning of the epidermis in *Caenorhabditis elegans*. *Genetics* **146**: 185–206.
- THOMAS, J. H., C. J. CEOL, H. T. SCHWARTZ and H. R. HORVITZ, 2003 New genes that interact with *lin-35* Rb to negatively regulate the *let-60* ras pathway in *Caenorhabditis elegans*. *Genetics* **164**: 135–151.
- VISINTIN, R., S. PRINZ and A. AMON, 1997 CDC20 and CDH1: a family of substrate-specific activators of APC-dependent proteolysis. *Science* **278**: 460–463.
- WANG, M., and P. STERNBERG, 2001 Pattern formation during *C. elegans* vulval induction. *Curr. Top. Dev. Biol.* **51**: 189–220.

Communicating editor: B. J. MEYER